Journal of Virological Methods 301 (2022) 114459

Contents lists available at ScienceDirect

Journal of Virological Methods

journal homepage: www.elsevier.com/locate/jviromet

Protocols

Differential detection of zika virus based on PCR

Daniel Alzate [a], Esteban Marín [b], Jahir Orozco [a], Carlos Muskus [b,*]

[a] Max Planck Tandem Group in Nanobioengineering, Institute of Chemistry, Faculty of Natural and Exact Sciencies, University of Antioquia, Complejo Ruta N, Calle 67 N° 52–20, Medellín, 050010, Colombia

[b] Programa de Estudio y Control de Enfermedades Tropicales (PECET), Facultad de Medicina, Universidad de Antioquia, Calle 62 N° 52-59, Medellín, Colombia

ARTICLE INFO

Keywords:
Zika virus
PCR
Diagnosis
Tropical diseases
Differential diagnosis

ABSTRACT

Tropical countries are highly prone to infectious diseases such as the one caused by zika virus. Infection by zika is clinically and epidemiologically highly relevant. For example, when women are infected by zika during the first trimester of pregnancy, the child incurs a high risk of microcephaly and acute neurological syndromes. In adults, the virus is associated with the Guillain-Barré syndrome and other disorders. The worldwide emergency caused by zika in 2013/14 demonstrated the need for rapid and accurate diagnostic tools for the virus. Current diagnostic methods include virus isolation, serological tests, and molecular assays. However, virus isolation requires labor-intensive and time-consuming cell culture; serological detection suffers from cross-reactivity caused by previous exposure to homologous arboviruses that cause symptoms like those caused by zika, while molecular tools commonly are not designed for differential zika detection. This work reports on developing a specific molecular detection method based on phylogenetically conserved primers designed for the specific diagnosis of the zika virus. The zika primers were systematically selected through a rigorous bioinformatic analysis and demonstrated the capability to be highly specific. We tested our primers on synthetic DNA, cell cultures and samples from patients infected with zika, dengue and chikungunya and found that they detected zika with specificity high enough for differential virus diagnosis.

1. Introduction

Zika virus is an arbovirus that belongs to the family Flaviviridae (Musso and Gubler, 2016). Its genome consists of approximately 10.800 nucleotides of a single-stranded RNA with positive polarity (Hasan et al., 2018; Kuno, 1998), packed into an icosahedral structure similar to other flaviviruses (Dai et al., 2016; Sirohi and Kuhn, 2017). The main vector for virus propagation is the mosquitoes of the genus *Aedes*, which spread the first great zika epidemic outbreak in Oceania between 2013/14. From there, the virus has likely spread throughout America between 2014/15 (Musso and Gubler, 2016) and compromised large areas of the Asian (Hu et al., 2019) and African (World Health Organization, 2019) continents, showing great epidemiological relevance.

Some of the frequent symptomatic manifestations of zika infection include fever, conjunctivitis, muscle and joint pain, although many patients do not manifest any symptoms (Calvet et al., 2016). Zika infection of women in the first trimester of pregnancy has a high probability of delivering children with microcephaly (Sikka et al., 2016; Rasmussen et al., 2016; Mlakar et al., 2016), a neurological development disorder that drastically reduces the size of the brain with severe reduction of cognitive function and intellectual capacity (Mlakar et al., 2016; Rasmussen et al., 2016). This can be accompanied by spasticity, craniofacial disproportion, miscarriage, and ocular abnormalities (Zhang et al., 2021). A preliminary case-control study showed that pregnant mothers infected with Zika virus were 8.6 times more likely to have a child with microcephaly than uninfected mothers (De Araújo et al., 2016). Zika Infection has also been probed to cause Guillain-Barre syndrome (Zhang et al., 2021; Cao-Lormeau et al., 2016), meningoencephalitis (Carteaux et al., 2016), myelitis (Mécharles et al., 2016) and ophthalmological abnormalities in infected adults (Fernandez et al., 2017). Apparently, the virus infects different cell types by different mechanisms where the envelope glycoprotein interacts with cell surface receptors such as DC-SIGN, AXL, TYRO3 and TIM-1 (Zhang et al., 2021).

Clinical and epidemiologic management of zika infections needs the availability of good diagnostic tests that can differentiate zika from other related viruses, given that some clinical indicators do not always lead to correct diagnosis with enough accuracy. Conventional diagnosis of zika relies on virus isolation upon infection of cell cultures, serological

* Corresponding author.
E-mail address: carlos.muskus@udea.edu.co (C. Muskus).

https://doi.org/10.1016/j.jviromet.2022.114459
Received 28 July 2021; Received in revised form 15 December 2021; Accepted 5 January 2022
Available online 7 January 2022

tests, and molecular assays such as nucleic acid amplification-based techniques (Digoutte et al., 1992; Hayes, 2009; Lanciotti et al., 2008a; Charrel et al., 2016). However, all these methods have drawbacks. Cell culture is labor-intensive and time-consuming. Serological detection suffers from cross-reactivity due to previous exposure to close phylogenetically related arboviruses or viruses with high sequence identity that produce similar symptoms, and molecular diagnostic tools are not precisely designed for differential zika virus detection or even for the detection of different lineages. Although no relevant evidence of cross-reactivity between Zika and Chikungunya (Chik) has been reported, there is evidence of cross-reaction between dengue and Chik [Kam et al., 2015], thus suggesting that cross-reaction may also occur with other flaviviruses, including zika. Regarding molecular tests, we have found that some PCR primers used for diagnostic purposes nonspecifically might amplify these two arboviruses which are transmitted by the same vector and cause similar clinical symptoms. For that, analysis of the published and widely used primers (Lanciotti et al., 2008b; Camacho et al., 2016; Faye et al., 2008; Calvo et al., 2016; Waggoner et al., 2016a; Grard et al., 2014; Kuno and Chang, 2007) with the nucleotide Blast algorithm (https://blast.ncbi.nlm.nih.gov), predicted a high probability that these primers will result in false-positive PCR when in fact other arbovirus is present, thus hindering the specific zika virus detection (data not shown).

Differential detection of zika virus was attempted by isothermal nucleic acid amplification using two specific primers to detect femtomolar virus concentrations (Pardee et al., 2016). Effectiveness of the method was probed by discriminating zika genome from three dengue serotypes. Subsequently, others applied methods such as RT-qPCR (Luis Eduardo Cuevas et al., 2016), reverse transcription loop-mediated isothermal amplification (RT-LAMP) (Priye et al., 2017; Song et al., 2016), triple reverse transcription real-time PCR (Pabbaraju et al., 2016), multiplexed reverse transcription real-time PCR (RT-PCR) (Waggoner et al., 2016b) and nano-biosensors (Alzate et al., 2020; Cajigas et al., 2020) have been developed. Importantly, Corman et al. (2016), showed that specificity of PCR-based tests is affected by recognition of polymorphic sequences by primers designed to target different regions of zika genome (Corman et al., 2016). Furthermore, specificity of some PCR tests may depend on zika lineage. Finally, detection limits vary among different primers, regions of the genome, and the virus lineage. For these reasons, some tests did not perform very well in clinical samples with low copy numbers, generating false-positive results (Corman et al., 2016).

Because the symptoms of zika, dengue and chikungunya are so similar, a diagnostic tool to differentiate among these agents would be indispensable. Using a rational and rigorous bioinformatic analysis, this work aims to design highly specific primers and probe their specificity, sensitivity, and ability to detect specifically zika infection. We demonstrate that our primers discriminated against synthetic target DNA, RNA both from virus-infected cell culture supernatants and from samples coming from patients infected by zika, dengue, and chikungunya viruses.

2. Materials and methods

2.1. Selection of conserved regions and primer design

Eight hundred ninety-one sequences from all zika-virus lineages reported worldwide until 2017 were downloaded from the NCBI database and filtered. A multi-fasta file was created with 117 final sequences after filtering based on a systematic review of each strain sequence to identify incomplete genomes, genomes with significant gaps, or genomes not isolated from humans. Sequences were loaded and aligned using the Clustal Omega program (McWilliam et al., 2013) to identify further the evolutionarily conserved regions by a consensus sequence analysis with Jalview (Waterhouse et al., 2009) and Bioedit (Hall, 1999) programs.

Specificity of the unique selected zika regions was confirmed by Blastn analysis against human, dengue, and chikungunya genomes. Selected target sequences were synthesized to evaluate their capability to discriminate zika from dengue and chikungunya by PCR.

The primers for each in silico selected zika-specific target region were designed by using Primer-BLAST (https://www.ncbi.nlm.nih.gov/tools/primer-blast/) and Primer3Plus (https://www.bioinformatics.nl/cgi-bin/primer3plus/primer3plus.cgi) programs. Primer thermodynamic parameters were analyzed with IDT Oligoanalyzer (Integrated DNA Technologies, https://www.idtdna.com/pages/tools/oligoanalyzer). Primer selection criteria mandated the length from 16-22-mers to provide high specificity and minimal probability of generating secondary structures or self-complementarity at sequence ends. Primer melting temperature (Tm) was to be similar with no more of 3 °C of differences. Guanine/cytosine (GC) content of primers was to be between 30–60 %. The last five nucleotides at the 3′ end of primers should not have had more than two G or C bases. Homopolymeric region of four or more identical nucleotides was avoided and the negative Gibbs free energy values were not to exceed scores higher than -8 kcal/mol to minimize the chance of homo-hetero dimers and hairpin structure formation.

2.2. Primer performance in conventional PCR with synthetic templates

Conventional PCR was set up with the four primer pairs and each of the four selected synthetic target DNA as templates. PCR reactions were run in a ProFlex thermocycler using the DreamTaq PCR master mix (2X) Kit (Thermo Scientific). The reaction was set with 12.5 μL of the 2X master mix, 1.5 μL of each primer solution at 5 μM, 4 μL (0.1 and 1 nmol/μL) of each synthetic DNA region (target region 1, 2, 5.1 and 5.2) at a concentration of 40 ng; the reaction was completed with up to 25 μL with RNAse-DNAse free water. The PCR cycling conditions were the following: initial denaturation cycle at 95 °C for 180 s, 30 cycles at 95 °C for 30 s; annealing temperature 52 °C (regions 1 and 2) or 59 °C (regions 5.1 and 5.2) for 30 s and extension at 72 °C for 30 s. A single final polymerization step was at 72 °C for 300 s. PCR products were electrophoresed in 2 % agarose gels for one h and stained with ethidium bromide. The gel was visualized in an E-Gel Imager System with UV Light Base (Thermo Scientific).

2.3. Performance of primers by RT-PCR

2.3.1. RNA extraction and reverse transcription

We used the Zymo Research ZR Viral RNA kit (https://www.zymoresearch.com/pages/viral-rna) to extract RNA (300−500 μL of input extraction sample) from supernatants of zika-infected cells *in vitro*, or from serum samples from zika-infected patients previously diagnosed by standard RT-PCR using commercially available primers at the lab where serum was obtained. RNA from zika-infected cells and serum samples was extracted following manufacturer's instructions. The reaction mix was always set in a laminar flow chamber sterilized with 70 % ethanol and UV irradiation for 30 min. Reverse transcription was conducted with the Thermo Scientific™ RevertAid™ First Strand cDNA Synthesis. For this, 1 μg of total RNA was mixed with 1 μL of Oligo (dT)18 primer and 1 μL of Random Hexamer primer, 4 μL of 5X buffer, 1 μL of RiboLock RNAse inhibitor (20 U/μL), 2 μL of 10 mM of dNTP mix, and 1 μL of Revert Aid M-MuL V RT enzyme (200 U/μL). The mix was centrifuged and incubated for 5 min at 25 °C followed by 60 min at 42 °C.

Specificity of primers for zika was also evaluated on cDNA retrotranscribed from RNA extracted from cell culture supernatants infected with dengue and chikungunya viruses. The RNA was extracted as described below. Specificity was evaluated by both conventional RT-PCR and real-time PCR.

2.3.2. Conventional reverse-transcription PCR

After RNA extraction, RT-PCR was carried out using the Verso SYBR Green 1-Step qRT-PCR Kit (Thermo Scientific) with samples obtained

from zika-infected cells and serum samples. RT-PCR was carried out according to manufacturer's instructions.

2.3.3. Electrophoresis of PCR products

PCR products obtained by PCR on synthetic DNA templates and by conventional RT-PCR using supernatant of zika-infected cell cultures and serum samples were run on 3 % agarose gel electrophoresis, stained with 0.5 μg/mL ethidium bromide and visualized in an E-Gel Imager (Thermo Fisher Scientific). Electrophoresis was run at 90 V for 40 min. A 100 bp DNA Ladder molecular weight marker (NorGen) was employed to determine the amplicon size. A 4 % agarose gel electrophoresis was also performed using hyperLadder V (500-25) bp marker for the development of amplified samples from zika-infected cell cultures (ZC) and cultures infected with dengue (DC) and chikungunya (CC) viruses. Electrophoresis was run at 80 V for 90 min, developed with the hydragreen DNA dye, and visualized with the E-Gel Imager.

2.4. Real time-PCR

A real-time PCR was run for the synthetic DNA targets and a RT-PCR was conducted for RNA obtained from cell-culture supernatants using the Two-step RT-PCR kit (Thermo Scientific). The reaction mix for the real time PCR was set up with the QuantiTect SYBR® Green PCR Kits using 12.5 μL of the master mix and 0.2 μM of each primer and 2 μL of the synthetic DNA targets. The final volume was complete up to 25 μL with DNAse free water. The RT- PCR was prepared in a total volume of 25 μL and contained 1.5 μL of each primer solution at 5 μM, 5.5 μL of nuclease-free water, 4 μL of the RNA sample and 12.5 μL of master mix (2X) containing 0.05 U/μL Taq DNA polymerase, 4 mM $MgCl_2$ and 0.2 mM of each deoxynucleotide. Negative (nuclease-free water) and positive (RNA purified from viral culture supernatants) were included in each run as controls.

Real-time PCR of patient serum samples was conducted using the Verso SYBR Green 1-Step qRT-PCR Kit (Thermo Scientific). The reaction was set up with 12.5 μL of one-step qPCR SYBR mix, 0.25 μL the Verso enzyme, 1.25 μL of the RT-enhancer, 0.5 μL (0.2 μM) of each forward and reverse primers, 4 μL of purified RNA and nuclease-free water up to 25 μL. All reactions were carried out in 0.2 mL PCR tubes in a QuantStudio 3 thermocycler (Thermo Scientific). The cycling conditions were like the conditions described for synthetic DNA templates, except than the reaction was run for 60 cycles.

2.5. Limit of detection

An aliquot of each of the synthetic DNAs corresponding to the R1 and R2 regions were quantified by fluorometry using a qubit (Thermo Fisher Scientific). With the DNA concentration, the number of copies was established, using the DNA copy number calculator program of the URI Genomics & Sequencing Center (https://cels.uri.edu/gsc/cndna.html). Once the number of copies was established, a 10-fold dilutions serie were made from 100,000 to 1 copy. The PCR was run as described in Materials and Methods in Section 2.2. The linear regression curve was calculated in Excel using the Ct values obtained for each number of copies of the synthetic DNAs.

2.6. Patient serum samples and supernatants of virus isolates

Samples of patient serum were kindly donated by the Instituto de Investigaciones Biológicas del Trópico (Universidad de Cordoba) in the city of Monteria-Colombia. Two supernatants of virus isolates were kindly donated by the Center for Research in Tropical Diseases (Universidad Industrial de Santander); from the Department of Santander, Colombia.

3. Results

3.1. Primer design

To identify the conserved sequences unique to zika virus genome, we aligned 117 zika genomes and compared them to human, dengue and chikungunya genomes using Nucleotide-BLAST. The analysis revealed ten such sequences ranging in size from 42 to 75 nucleotides. These ten sequences were used to design the primers using Primer-BLAST and Primer3Plus programs, but only three sequences (Table 1) allowed the design of highly specific primers. We named the sequences Region 1 (R1), Region 2 (R2), and Region 5 (R5). However, for the purpose of primer design, region 5 was divided into two subregions, R5.1 and R5.2. The selected primer list and their target sequences (amplicons) are shown in Table 2.

The alignment of specific nucleotide sequences is important because it provides valuable information for knowing the phylogenetic relationships traced by the species' evolutionary history and because conserved portions of the genome have physiological and adaptative implications. The conserved zika sequences were mapped into the reference zika virus isolate PRVABC59 reference genome (https://www.ncbi.nlm.nih.gov/nuccore/MH158237); (Table 3 and Scheme S1). This analysis revealed the sequences within the zika genome that are highly conserved and their corresponding target genes.

Based on nucleotide sequences size, the extent of the untranslated regions of the virus (5′ and 3′ UTRs), the size and position of the sequences encoding the unique polyprotein of the zika virus within the global genome, as well as the positions of the sequences encoding the structural and non-structural proteins of the virus, it was possible to track the location of the conserved and specific regions of the virus that were obtained by bioinformatic analyses. Table 3 summarizes the results of the genetic mapping.

It is important to highlight that the R1 and R2 regions are located in the non-structural protein 5 (NS5), where key residues and the structural motifs of methyltransferase and viral RNA polymerase are located (Zhao et al., 2017). These results highlight the functional implications of the sequences found through computational biology algorithms in the zika virus genome. The NS5 RNA-dependent RNA polymerase (RdRp) is a flaviviral non-structural protein that has a central role in replicating the zika virus genome and is absent in mammalian hosts, a relevant target drug discovery. Therefore, active ingredients that are inhibitors of NS5 RdRp, especially molecules directed to the so-called priming loop that regulates the RNA template's binding and the virus's polymerization process, have been vigorously sought. (Zhao et al., 2017; Godoy et al., 2017). The priming loop is responsible for the allosteric positioning of the 3′end of the RNA template at the active site of the RdRp in the zika virus. In summary, the NS5 proteins of the dengue and zika viruses differ in the network of molecular interactions and the orientations of the methyltransferase (MT) and RdRp domains (Zhao et al., 2017). Interestingly, the R2 conserved zika sequence showed the best PCR performance, which amplified a region located at the beginning of the NS5 gene.

The conserved sequences of R1 correspond to the priming loop, which performs stacking by interacting with the initiating nucleotide in the polymerase catalytic pocket. The priming loop is located in the subthumb domain deployed within the catalytic chamber to promote the initiation complex formation (Duan et al., 2017). The R1 and R2 sequences correspond to the amplified regions of the molecular targets located in the region that codes for the priming loop and loop four of the palm that composes the virus polymerase. R5.1 and R5.2 correspond to the amplified regions of the molecular targets that are located in the 3′end region of the virus genome that is not translated into proteins.

3.2. Primers testing by conventional PCR

We tested our primers using synthetic DNA targets according to the

Table 1
Conserved regions of the zika virus that allowed the design of highly specific primers.

Regions	Sequences (5′→3′)	NTs	Genome coordinates
R1	TCATCTGTGCCAGTTGATTGGGTTCCAACTGGGAGAACTACCTGGTCAATCCATGGAAAGGGAGAATGGATGACCA	**76**	**10342-10417**
R2	ATGGGAAAAAGAGAAAAGAAACAAGGGGAATTTGGAAAGGCCAAGGGCAGCCGCGCCATCTGGTATATGTGGC	**73**	**9361-9434**
R5	AAAAGCAACACCATAAAAAGTGTGTCCACCACGAGCCAGCTCCTCTTGGGGCGCATGGACGGGCC	**65**	**8671-8735**

Table 2
List of zika primers selected and their specific target sequences.

Region	Primers Forward (5′→3′)	Primers Reverse (5′→3′)
R1	ACTGGGAGAACTACCTGGTC	GGTCATCCATTCTCCCTTTCC
R1 Amplicon	ACTGGGAGAACTACCTGGTCAATCCATGGAAAGGGAGAATGGATGACC	
R2	CAAGGGGAATTTGGAAAGGC	GCCACATATACCAGATGGCG
R2 Amplicon	CAAGGGGAATTTGGAAAGGCCAAGGGCAGCCGCGCCATCTGGTATATGTGGC	
R5.1	GTGTCCACCACGAGCCAG	CATGCGCCCCAAGAGGAG
R5.1 Amplicon	GTGTCCACCACGAGCCAGCTCCTCTTGGGGCGCATG	
R5.2	TCCACCACGAGCCAGCTC	GTCCATGCGCCCCAAGAG
R5.2 Amplicon	TCCACCACGAGCCAGCTCCTCTTGGGGCGCATGGAC	

Table 3
Genetic mapping of conserved sequences of the zika virus that allow the design of optimal primers.

Conserved sequence	Coding	Non-coding	Position within the genome	Domain/ subdomain
R1	X		NS5	*Thumb/Priming Loop*
R2	X		NS5	*Palm/Loop 4*
R5,1		X	UTR 3′	–
R5,2		X	UTR 3′	–

sequence of the four unique zika-virus genome regions (Table 2) and RNA extracted from supernatants of cell cultures infected individually by zika, dengue, and chikungunya viruses and reversely transcribed. PCR products for each pair of primer and synthetic target DNA were amplified by the conventional PCR protocol (Fig. S1a). Electrophoresis of the respective PCR products is shown in Fig. 1a; lines 3 and 4; it demonstrates that PCR amplifies exclusively with the synthetic DNA zika targets and zika-virus supernatants, but not with the supernatants of cells infected with dengue or chikungunya viruses (Fig. 1a lines 1 and 2). In addition, the PCR products specific for zika were of the expected size for each of the four identified unique zika genome regions.

To optimize the annealing temperatures for each of the four zika region, we determined their annealing effectiveness at different temperatures (Figs. 1b and S2). The annealing temperature range was set up four centigrades below and above of the primers' Tm. For the region R1, we obtained Tm = 55 °C; for R2, Tm = 49 °C; for R5.1 and R5.2, Tm = 60 °C. These were the annealing temperature used in subsequent PCR reactions.

3.3. Primers testing by real time PCR

To obtain further insight into the characteristics of the four set of primers, we also employed real-time PCR; sensitivity of the method would facilitate detection of cross-reactivity with other templates (Corman et al., 2016). Fig. 2 shows the data obtained with the R1 primers and the corresponding synthetic DNA, viral supernatant extracts from zika, dengue and chikungunya, and negative control. The primers R1 amplified exclusively the synthetic DNA target and cDNA derived from zika virus as demonstrated by the obtention of the same melting temperature (inset box in Fig. 2), while other two viral extracts (dengue and chikungunya) did not; thus, demonstrating the specificity of the R1 primers. The primer pairs for R2, R.5.1 and R5.2, also showed a similar amplification performance (See the amplification and melting curves in the Fig. S3 of the supplementary material). Primers for R1 and R2

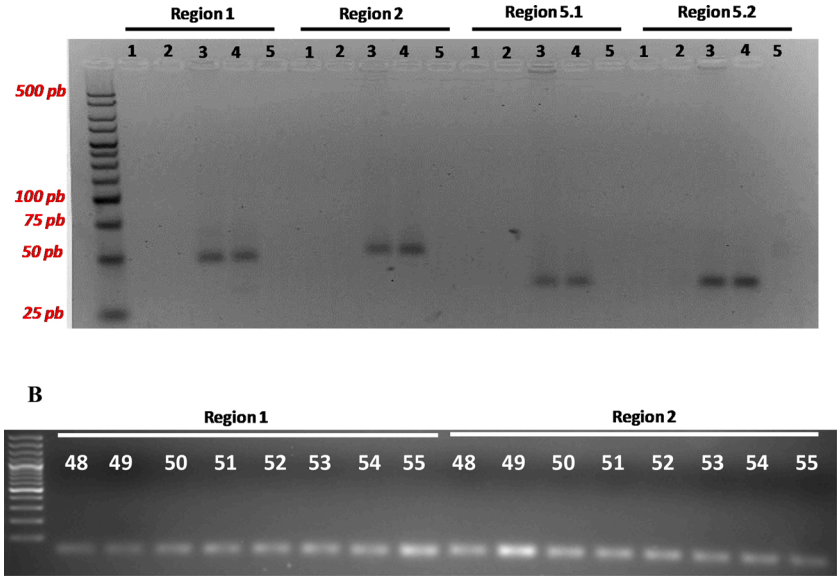

Fig. 1. Performance and specificity of the moleculardesigned primers. Agarose gel electrophoresis of the products amplified by conventional PCR. A) PCR products amplified from supernatants of infected cell cultures (the first step was converting the RNA from the cultures in the cDNA for further amplification). Dengue (line1), chikungunya (line 2), zika (line 3), zika synthetic target DNA for each primers pair (line 4) and negative control (line 5). All negative controls included nuclease-free water instead of genetic material. The synthetic regions and cell cultures amplification of zika virus were highly specific. B) Temperature gradient for the primers, in °C.

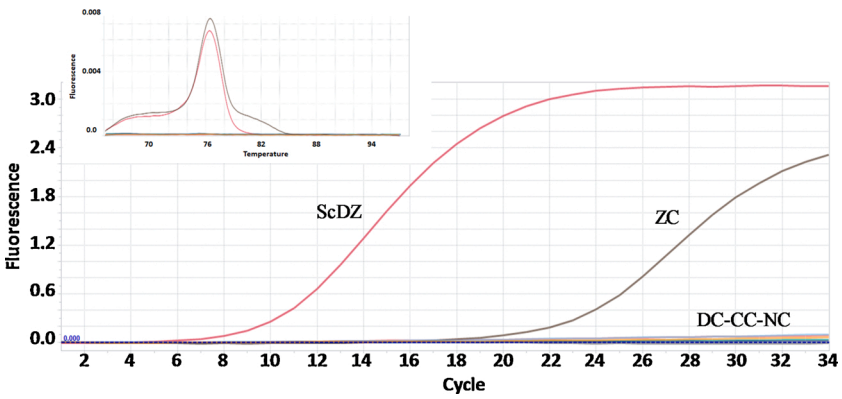

Fig. 2. Amplification of RNA extracted from supernatants of zika, dengue and chikungunya virus-infected cells by real-time PCR using primers for R1. Amplification curves were observed for the corresponding synthetic target and supernatant of zika virus-infected cells (the first step for each virus was converting the RNA extracted from the cell cultures to the cDNA for further amplification). The same melting curves were obtained for both templates, Tm = 76 (inner inset). ScDZ, synthetic DNA of the R1; ZC, RNA from zika virus-infected cells; DC, RNA from dengue virus-infected cells; CC, RNA from chikungunya virus-infected cells and NC, negative control.

regions were preferred to evaluate the clinical samples because of the size of the amplicon generated in the PCR. Primers for R1 and R2 regions amplify a 48 and 52 bp products, in contrast with the smaller products of 36 bp amplified with the primers for region 5.1 and 5.2, which could be confused with primer-dimers in conventional PCR and visualized in gel electrophoresis.

Once the performance of the primers was validated with synthetic DNA and reverse transcribed RNA obtained from supernatants of zika, dengue and chikungunya-infected cells, next, we set to determine the diagnostic potential of our primers by evaluating them in the sera of 15 zika-infected patients from the city of Monteria and two supernatants from zika-infected cells from the Department of Santander. The Monteria's samples were provided to us encoded as D485, D589, D588, D586, D533, D511 and D479 (cohort I) and AM1, AM5, AM12, AM13, AM23, AM27, AM30 and AM34 (cohort II). The two supernatants from Santander, were identified as D016 and D109. A single PCR product was obtained from each fifteen sera using primers for R1 region (upper panel of Fig. 3 and inner inset) and primers for R2 region (lower panel of Fig. 3 and inner inset). The amplification of the remaining samples from Monteria and Santander are showed in Supplementary Fig. S4. These results suggest again a good PCR specificity at least again dengue and chikungunya virus. However, in silico Blast analysis of specificity of the primers (due to the lack of clinical samples infected with arboviruses genetically close to Zika) showed that the primers are also specific when analyzing against yellow fever, west nile and St Louis encephalitis genomes (data not shown). The different threshold-cycle (Ct) values obtained for the fifteen clinical samples from Monteria and the two supernatants from Santander are detailed in Table 4.

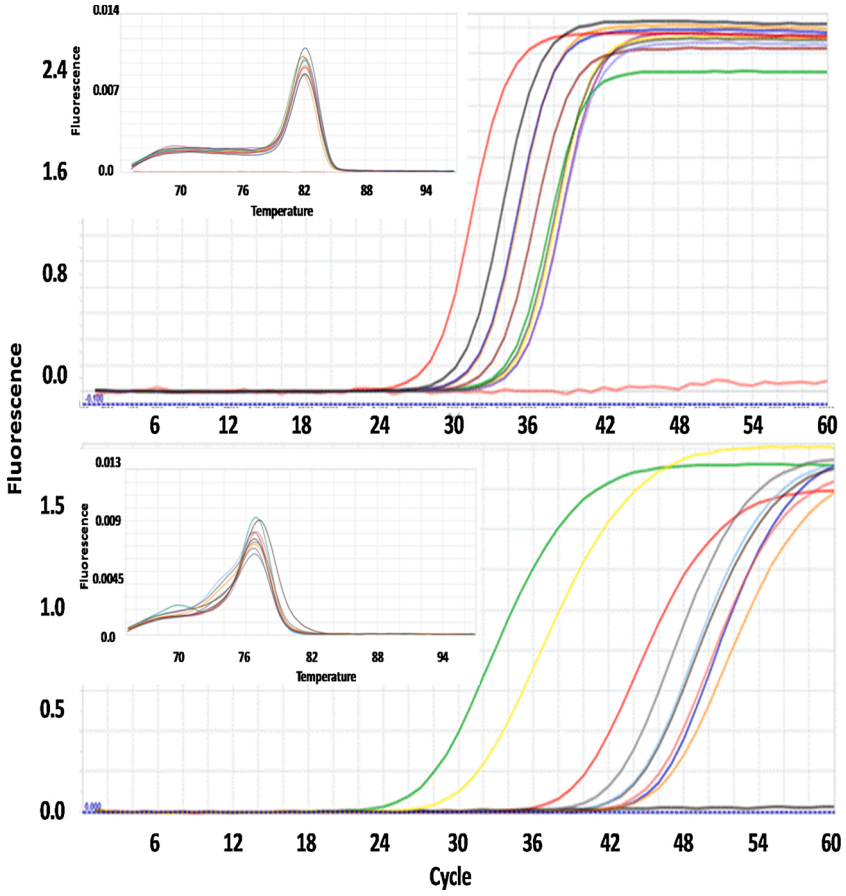

Fig. 3. Detection of RNA zika virus extracted of serum samples from infected patients by real-time PCR, using primers designed for the R2 region (upper panel) and R1 region (bottom panel) with the corresponding melting curves in the inner insets, Tm = 82 °C for R2 and 77 °C for R1, respectively.

Table 4
Threshold-cycle values (Ct) measured in serum samples of zika infected patients with R1 and R2 primers, respectively. Statistical analysis by Student's *t*-test for unpaired samples. Probability that the two groups were statistically indistinguishable is $p < 0.0001$.

Sample	R1	R2
1	47.1	36.7
2	43.0	37.9
3	44.7	36.9
4	44.8	39.7
5	46.1	40.2
6	46.6	41.9
7	40.2	34.2
8	28.1	21.8
9	31.5	23.8
10	43.6	34.4
11	41.4	35.0
12	41.6	32.8
13	43.1	34.1
14	41.6	34.7
15	36.8	31.4
16	45.9	35.0
17	39.8	31.5
18	45.2	30.2
19	40.9	27.7
Mean ± SD	**41.7 ± 5.0**	**33.7 ± 5.2**

The Ctould be employed as a measure of analytical sensitivity, where the lower the Ct value the higher the analytical sensitivity (de Moraes et al., 2018). To compare the characteristics of R1 and R2 primer sets, we analyze the Ct obtained with the two primer sets in the 15 clinical samples and two supernatants. Data in Table 4 demonstrate lower Ct values for products amplified with R2 primers (Mean ± SD)33.7 ± 5.2 than with R1 primers 41.7 ± 5.1; $p < 0.0001$) indicating better limit of detection for the R2 primers. This conclusion is in line with the empirical LOD estimated to be 1 copy/μL ($R^2 = 0.99$) and 1 copy/μL ($R^2 = 0.97$), supplementary (Figs. 4 and 5). This detection limit is quite good and was close to the LOD of the real-time RT-PCR approach and it behaves better or similar to some of the RT-PCRs described for the diagnosis of Zika (Zhang et al., 2021). However, multiplex RT-PCRs for the simultaneous detection of Zika with other arboviruses have a slightly higher LOD (Mishra et al., 2019; Santiago et al., 2018), compromising some of sensitivity for the detection of several related pathogens at the same time.

Melting curves of the samples are similar to positive controls, the supernatants of cell culture infected with the zika virus, and the respective synthetic targets, hence suggesting again specificity of the reaction.

These results demonstrate that our primers, designed by the aid of a bioinformatic analysis, allow the specific detection of zika virus RNA with no amplification of dengue and chikungunya viruses. Particularly, our primers can be used in both, conventional or real-time PCR amplification with good sensitivity and specificity. The specificity was experimentally demonstrated against dengue and chikungunya and checked in silico against Yellow fever, West nile and St Louis encephalitis viruses (data not shown) so this assay can be used as a tool for differential diagnosis of zika-virus infection in sera samples, as the probability of false-positive results is virtually null.

4. Conclusion

We developed a molecular diagnostic test to detect the zika virus RNA based on new highly specific primers, which were able to discriminate very well against dengue and chikungunya homologous arboviruses. Primers were designed through a robust and rigorous bioinformatic analysis, whose specificity was also verified by bioinformatic analysis and confirmed by conventional and real-time PCR experiments, with synthetic DNA of four selected target regions and RNA extracted from virus-infected cells. Finally, we evaluated the primers and the diagnosis tool performance in sera obtained from confirmed infected patients. The primers designed to amplify the R2 conserved zika sequence presented the best performance. Although a complete validation of the tool is mandatory with a larger cohort of patients, the primers

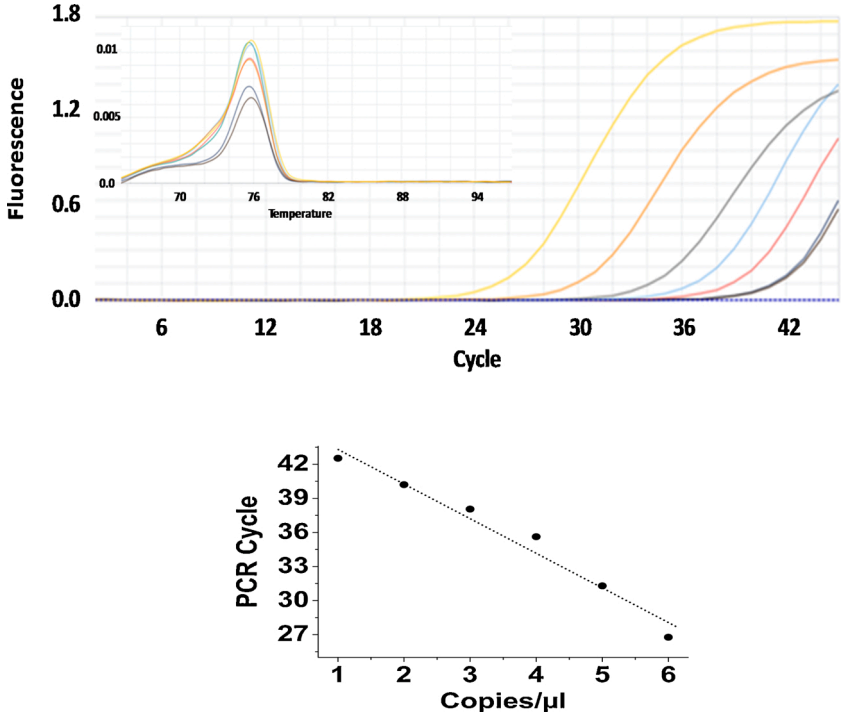

Fig. 4. Real-time PCR detection of synthetic zika virus DNA, amplified for different copy numbers with primers for R1 (upper panel). The inner inset corresponds to the melting curve for each PCR amplified product. The standard curve (lower panel) shows the specific value of the PCR cycle for each DNA copy number amplification, with a LOD of 1 copy/μL ($R^2 = 0.97$).

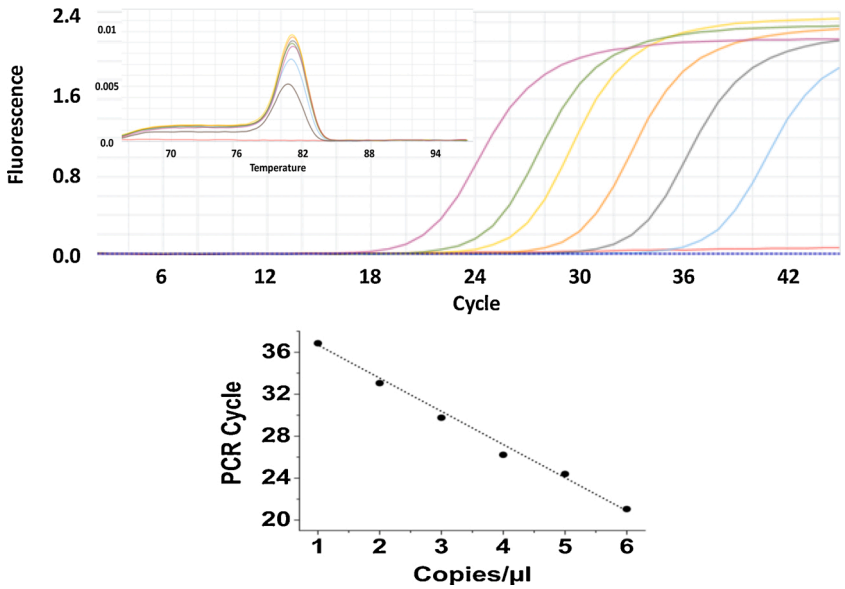

Fig. 5. Real-time PCR detection of synthetic zika virus DNA, amplified for different copy numbers with primers for R2 (upper panel). The inner inset corresponds to the melting curve for each PCR amplified product. The standard curve (lower panel) shows the specific value of the PCR cycle for each DNA copy number amplification, with a LOD of 1 copy/µL ($R^2 = 0{,}99$).

designed and tested in the developed molecular test can be implemented in the differential diagnosis of the zika virus, due to their very high specificity, with the potential to respond to epidemiological emergencies during a new zika outbreak.

Author summary

Currently, neither a zika-virus-specific treatment nor a zika-directed vaccine is available making clinical management of zika infection challenging. Methods nowadays used for detection regularly misdiagnose zika as dengue or chikungunya posing undue challenges to the clinician. Current diagnostic tests employ virus isolation requiring cell culture, serological tests and molecular assays. These methods have limitations; cell culture is time-consuming, serological tests can be cross-reactive with other flaviviruses, and current PCR methods use primers not sufficiently specific to avoid amplification of other flaviviruses. This situation urges the development of fast and reliable detection tools for diagnosing zika viral infection. In this work, we used bioinformatic tools to analyze zika-virus sequences and use the results to design highly specific PCR primers. By RT-qPCR we tested the primers on laboratory and clinical samples. We found that the method discriminates the zika virus from genetically homologous viruses such as dengue virus and other arboviruses like chikungunya and enables thus a differential diagnosis of zika virus in infected patients.

Data availability

No data was used for the research described in the article.
Data will be made available on request.

Declaration of Competing Interest

The authors declare that they have no known competing financial interests or personal relationships that could have appeared to influence the work reported in this paper.

Acknowledgements

The work has been funded by COLCIENCIAS, through the 111574454836 project. J.O thanks support from The University of Antioquia and The Max Planck Society through the cooperation agreement 566–1, 2014. Authors thank Dr. Raquel E. Ocazionez from The Medical School, Centro de Investigaciones en Enfermedades Tropicales (Universidad Industrial de Santander) and Dr. Salim Mattar, Instituto de Investigaciones Biológicas del Trópico IIBT (Universidad de Cordoba) for providing us with virus isolates and serum samples from infected patients, respectively.

Appendix A. Supplementary data

Supplementary material related to this article can be found, in the online version, at doi:https://doi.org/10.1016/j.jviromet.2022.114459.

References

Alzate, D., Cajigas, S., Robledo, S., Muskus, C., Orozco, J., 2020. Genosensors for differential detection of Zika virus. Talanta 210, 120648. https://doi.org/10.1016/j.talanta.2019.120648.

Cajigas, S., Alzate, D., Orozco, J., 2020. Gold nanoparticle/DNA-Based Nanobioconjugate for Electrochemical Detection of Zika Virus, pp. 1–10.

Calvet, G.A., Santos, F.B., Sequeira, P.C., 2016. Zika virus infection: epidemiology, clinical manifestations and diagnosis. Curr. Opin. Infect. Dis. 29 (October (5)), 459–466. https://doi.org/10.1097/QCO.0000000000000301.

Calvo, E.P., Sánchez-Quete, F., Durán, S., Sandoval, I., Castellanos, J.E., 2016. Easy and inexpensive molecular detection of dengue, chikungunya and zika viruses in febrile patients. Acta Trop. 163, 32–37. https://doi.org/10.1016/j.actatropica.2016.07.021.

Camacho, E., Paternina-Gomez, M., Blanco, P.J., Osorio, J.E., Aliota, M.T., 2016. Detection of autochthonous zika virus transmission in Sincelejo, Colombia. Emerg. Infect. Dis. 22, 927–929. https://doi.org/10.3201/eid2205.160023.

Cao-Lormeau, V.-M., Blake, A., Mons, S., Lastère, S., Roche, C., Vanhomwegen, J., Dub, T., Baudouin, L., Teissier, A., Larre, P., Vial, A.-L., Decam, C., Choumet, V., Halstead, S.K., Willison, H.J., Musset, L., Manuguerra, J.-C., Despres, P., Fournier, E., Mallet, H.-P., Musso, D., Fontanet, A., Neil, J., Ghawché, F., 2016. Guillain-Barré Syndrome outbreak associated with Zika virus infection in French Polynesia: a case-control study. Lancet 387, 1531–1539. https://doi.org/10.1016/S0140-6736(16)00562-6.

Carteaux, G., Maquart, M., Bedet, A., Contou, D., Brugi`eres, P., Fourati, S., Cleret de Langavant, L., de Broucker, T., Brun-Buisson, C., Leparc-Goffart, I., Mekontso Dessap, A., 2016. Zika virus associated with meningoencephalitis. N. Engl. J. Med. 374, 1595–1596.

Charrel, R.émi N., Leparc-Goffart, Isabelle, Pas, Suzan, de Lamballerie, Xavier, Koopmans, Marion, Reusken, Chantal, 2016. Background review for diagnostic test development for Zika virus infection. Bull. World Health Organ. 94 (August (8)), 574D–584D. https://doi.org/10.2471/BLT.16.171207.

Corman, V.M., Rasche, A., Baronti, C., et al., 2016. Assay optimization for molecular detection of Zika virus. Bull. World Health Organ. 94 (12), 880–892.

Dai, L., Song, J., Lu, X., Deng, Y.Q., Musyoki, A.M., Cheng, H., Zhang, Y., Yuan, Y., Song, H., Haywood, J., Xiao, H., Yan, J., Shi, Y., Qin, C.F., Qi, J., Gao, G.F., 2016. Structures of the zika virus envelope protein and its complex with a flavivirus broadly protective antibody. Cell Host Microbe 19, 696–704. https://doi.org/10.1016/j.chom.2016.04.013.

De Araújo, T.V.B., Rodrigues, L.C., de Alencar Ximenes, R.A., de Barros Miranda-Filho, D., Montarroyos, U.R., de Melo, A.P.L., Valongueiro, S., de Albuquerque, M.d. F.P.M., Souza, W.V., Braga, C., et al., 2016. Association between Zika virus infection and microcephaly in Brazil, January to May, 2016: preliminary report of a case-control study. Lancet Infect. Dis. 16, 1356–1363.

de Moraes, F.M., Espósito, D.L.A., Klein, T.M., da Fonseca, B.A.L., 2018. Searching for the best real-time RT-PCRs to detect Zika virus infections: the importance of comparing several protocols. Braz. J. Med. Biol. Res. 51 (6), e7221 https://doi.org/10.1590/1414-431X20187221.

Digoutte, J.P., Calvo-Wilson, M.A., Mondo, M., Traore-Lamizana, M., Adam, F., 1992. Continuous cell lines and immune ascitic fluid pools in arbovirus detection. Res. Virol. 143 (6), 417–422.

Duan, W., Song, H., Wang, H., Chai, Y., Su, C., Qi, J., Shi, Y., Gao, G.F., 2017. The crystal structure of Zika virus NS5 reveals conserved drug targets. EMBO J. 36, 919–933. https://doi.org/10.15252/embj.201696241.

Faye, O., Faye, O., Dupressoir, A., Weidmann, M., Ndiaye, M., Alpha Sall, A., 2008. One-step RT-PCR for detection of Zika virus. J. Clin. Virol. 43, 96–101. https://doi.org/10.1016/j.jcv.2008.05.005.

Fernandez, M.P., Saad, E.P., Martinez, M.O., Corchuelo, S., Reyes, M.M., Herrera, M.J., Saavedra, M.P., Rico, A., Fernandez, A.M., Lee, R.K., Ventura, C.V., Berrocal, A.M., Dubovy, S.R., 2017. Ocular Histopathologic Features of Congenital Zika Syndrome, pp. 1–7. https://doi.org/10.1001/jamaophthalmol.2017.3595.

Godoy, A.S., Lima, G.M.A., Oliveira, K.I.Z., Torres, N.U., Maluf, F.V., Guido, R.V.C., Oliva, G., 2017. Crystal structure of Zika virus NS5 RNA-dependent RNA polymerase. Nat. Commun. 8, 1–6. https://doi.org/10.1038/ncomms14764.

Grard, G., Caron, M., Mombo, I.M., Nkoghe, D., Mboui Ondo, S., Jiolle, D., Fontenille, D., Paupy, C., Leroy, E.M., 2014. Zika virus in Gabon (Central Africa) - 2007: a new threat from *Aedes albopictus*? PLoS Negl. Trop. Dis. 8, 1–6. https://doi.org/10.1371/journal.pntd.0002681.

Hall, T.A., 1999. BioEdit: a user-friendly biological sequence alignment editor and analysis program for Windows 95/98/NT. Nucl. Acids. Symp. Ser. 41, 95–98.

Hasan, S.S., Sevvana, M., Kuhn, R.J., Rossmann, M.G., 2018. Structural biology of Zika virus and other flaviviruses. Nat. Struct. Mol. Biol. 25, 13–20. https://doi.org/10.1038/s41594-017-0010-8.

Hayes, E.B., 2009. Zika virus outside Africa. Emerg Infect Dis. 15 (September (9)), 1347–1350.

Hu, Tao, Li, Juan, Carr, Michael J., Duchene, Sebastian, Shi, Weifeng, 2019. The Asian lineage of Zika virus: transmission and evolution in Asia and the Americas, 2019 Virol. Sin. 34, 1–8. https://doi.org/10.1007/s12250-018-0078-2.

Kam, Y.W., Pok, K.Y., Eng, K.E., Tan, L.K., Kaur, S., et al., 2015. Sero-prevalence and cross-reactivity of Chikungunya virus specific anti-E2EP3 antibodies in arbovirus-infected patients. PLoS Negl. Trop. Dis. 9 (1), e3445 https://doi.org/10.1371/journal.pntd.0003445.

Kuno, G., 1998. Universal diagnostic RT-PCR protocol for arboviruses. J. Virol. Methods 72, 27–41. https://doi.org/10.1016/S0166-0934(98)00003-2.

Kuno, G., Chang, G.J.J., 2007. Full-length sequencing and genomic characterization of Bagaza, Kedougou, and Zika viruses. Arch. Virol. 152, 687–696. https://doi.org/10.1007/s00705-006-0903-z.

Lanciotti, R.S., Kosoy, O.L., Laven, J.J., Velez, J.O., Lambert, A.J., Johnson, A.J., Stanfield, S.M., Duffy, M.R., 2008a. Genetic and serologic properties of Zika virus associated with an epidemic, Yap State, Micronesia, 2007. Emerg. Infect. Dis. 14 (August (8)), 1232–1239.

Lanciotti, R.S., Kosoy, O.L., Laven, J.J., Velez, J.O., Lambert, A.J., Johnson, A.J., Stanfield, S.M., Duffy, M.R., 2008b. Genetic and serologic properties of Zika virus associated with an epidemic, Yap State, Micronesia, 2007. Emerg. Infect. Dis. 14, 1232–1239. https://doi.org/10.3201/eid1408.080287.

Luis Eduardo Cuevas, E.A., Edge, David, Gurgel, Ricardo Queiroz, Edwards, T., Lalloo, D., 2016. Zika: novel point-of-care molecular diagnostics for the simultaneous diagnosis of Zika, chikungunya and dengue infections in Latin America. Liverpool Sch. Trop. Med. http://gtr.rcuk.ac.uk/projects?ref=MC_PC_15089.

McWilliam, H., Li, W., Uludag, M., Squizzato, S., Park, Y.M., Buso, N., Cowley, A.P., Lopez, R., 2013. Analysis tool web services from the EMBL-EBI. Nucleic Acids Res. 41 (July (Web Server issue)), W597–W600. https://doi.org/10.1093/nar/gkt376), 2013.

Mécharles, S., Herrmann, C., Poullain, P., Tran, T.H., Deschamps, N., Mathon, G., Landais, A., Breurec, S., Lannuzel, A., 2016. Acute myelitis due to Zika virus infection. Lancet 387, 1481.

Mishra, Nischay, Ng, James, Rakeman, Jennifer L., Perry, Michael J., Centurioni, Dominick A., Dean, Amy B., Price, Adam, Thakkar, Riddhi, Angus, Andreina Garcia, Williamson, Phillip, Delwart, Eric, Carrington, Christine, Sahadeo, Nikita, Che, Xiaoyu, Briese, Thomas, Tokarz, Rafal, Ian Lipkin, W., 2019. One-step pentaplex real-time polymerase chain reaction assay for detection of Zika, Dengue, Chikungunya, West Nile viruses and a human housekeeping gene. J. Clin. Virol. 120, 44–50. https://doi.org/10.1016/j.jcv.2019.08.011.

Mlakar, Jernej, Korva, Misa, Tul, Nataša, Popović, Mara, Poljšak-Prijatelj, Mateja, Mraz, Jerica, Kolenc, Marko, Rus, Katarina Resman, Vipotnik, Tina Vesnaver, Vodušek, Vesna Fabjan, Vizjak, Alenka, Pižem, Jože, Petrovec, Miroslav, Županc, Tatjana Avšič, 2016. Zika virus associated with microcephaly. N. Engl. J. Med. 374, 951–958. https://doi.org/10.1056/NEJMoa1600651.

Musso, Didier, Gubler, Duane J., 2016. Zika viruses. Clin. Microbiol. Rev. 3 (29), 488–524. https://doi.org/10.1128/CMR.00072-15.

Pabbaraju, K., Wong, S., Gill, K., Fonseca, K., Tipples, G.A., Tellier, R., 2016. Simultaneous detection of Zika, Chikungunya and Dengue viruses by a multiplex real-time RT-PCR assay. J. Clin. Virol. 83, 66–71. https://doi.org/10.1016/j.jcv.2016.09.001.

Pardee, K., Green, A.A., Takahashi, M.K., Braff, D., Lambert, G., Lee, J.W., Ferrante, T., Ma, D., Donghia, N., Fan, M., Daringer, N.M., Bosch, I., Dudley, D.M., O'Connor, D. H., Gehrke, L., Collins, J.J., 2016. Rapid, low-cost detection of Zika virus using programmable biomolecular components. Cell 165, 1255–1266. https://doi.org/10.1016/j.cell.2016.04.059.

Priye, A., Bird, S.W., Light, Y.K., Ball, C.S., Negrete, O.A., Meagher, R.J., 2017. A smartphone based diagnostic platform for rapid detection of Zika, chikungunya, and dengue viruses. Sci. Rep. 7, 1–11. https://doi.org/10.1038/srep44778.

Rasmussen, S.A., Jamieson, D.J., Honein, M.A., Petersen, L.R., 2016. Zika virus and birth defects — reviewing the evidence for causality. N. Engl. J. Med. 374, 1981–1987. https://doi.org/10.1056/nejmsr1604338.

Santiago, Gilberto A., Vázquez, Jesús, Courtney, Sean, Matías, Katia Y., Andersen, Lauren E., Colón, Candimar, Butler, Angela E., Roulo, Rebecca, Bowzard, John, Villanueva, Julie M., Muñoz-Jordan, Jorge L., 2018. Performance of the Trioplex real-time RT-PCR assay for detection of Zika, dengue, and chikungunya viruses. Nat. Commun. 9, 1391. https://doi.org/10.1038/s41467-018-03772-1.

Sikka, Veronica, Chattu, Vijay Kumar, Popli, Raaj K., Galwankar, Sagar C., Kelkar, Dhanashree, Sawicki, Stanley G., Stawicki, Stanislaw P., Papadimos, Thomas J., 2016. The emergence of Zika virus as a global health security threat: a review and a consensus statement of the INDUSEM joint working group (JWG). J. Glob. Infect. Dis. 8, 3–15.

Sirohi, D., Kuhn, R.J., 2017. Zika virus structure, maturation, and receptors. J. Infect. Dis. 216, S935–S944. https://doi.org/10.1093/infdis/jix515.

Song, J., Mauk, M.G., Hackett, B.A., Cherry, S., Bau, H.H., Liu, C., 2016. Instrument-free point of care molecular detection of Zika virus. Anal. Chem. 88, 7289–7294. https://doi.org/10.1021/acs.analchem.6b01632.

Waggoner, J.J., Gresh, L., Mohamed-Hadley, A., Ballesteros, G., Vargas Davila, M.J., Tellez, Y., Sahoo, M.K., Balmaseda, A., Harris, E., Pinsky, B.A., 2016a. Single-reaction multiplex reverse transcription PCR for detection of zika, chikungunya, and dengue viruses. Emerg. Infect. Dis. 22, 1295–1297. https://doi.org/10.3201/eid2207.160326.

Waggoner, Jesse J., Gresh, Lionel, Mohamed-Hadley, Alisha, Ballesteros, Gabriela, Davila, Maria Jose Vargas, Tellez, Yolanda, Sahoo, Malaya K., Balmaseda, Angel, Harris, Eva, 2016b. Single - reaction multiplex reverse transcription PCR for detection of Zika, Chikungunya, and Dengue viruses. Emerg. Infect. Dis. 22, 1295–1297.

Waterhouse, A.M., Procter, J.B., Martin, D.M.A., Clamp, M., Barton, G.J., 2009. Jalview Version 2-a multiple sequence alignment editor and analysis workbench. Bioinformatics 25, 1189–1191. https://doi.org/10.1093/bioinformatics/btp033.

World Health Organization, 2019. Zika Epidemiological Updates. July, Accessible at: https://www.who.int/emergencies/diseases/zika/zika-epidemiology-update-july-2019.pdf.

Zhang, X., Li, G., Chen, G., Zhu, N., Wu, D., Wu, Y., James, T.D., 2021. Recent progresses and remaining challenges for the detection of Zika virus. Med. Res. Rev. 41 (4), 2039–2108. https://doi.org/10.1002/med.21786.

Zhao, B., Yi, G., Du, F., Chuang, Y.C., Vaughan, R.C., Sankaran, B., Kao, C.C., Li, P., 2017. Structure and function of the Zika virus full-length NS5 protein. Nat. Commun. 8, 1–9. https://doi.org/10.1038/ncomms14762.